NEUROIMAGE **6,** 279–287 (1997)
ARTICLE NO. NI970303

Parametric Imaging of Ligand-Receptor Binding in PET Using a Simplified Reference Region Model

Roger N. Gunn,* Adriaan A. Lammertsma,† Susan P. Hume,* and Vincent J. Cunningham*

**PET Methodology Group, MRC Cyclotron Unit, Hammersmith Hospital, London, United Kingdom; and †PET Centre, Free University Hospital, Amsterdam, Netherlands*

Received February 10, 1997

A method is presented for the generation of parametric images of radioligand–receptor binding using PET. The method is based on a simplified reference region compartmental model, which requires no arterial blood sampling, and gives parametric images of both the binding potential of the radioligand and its local rate of delivery relative to the reference region. The technique presented for the estimation of parameters in the model employs a set of basis functions which enables the incorporation of parameter bounds. This basis function method (BFM) is compared with conventional nonlinear least squares estimation of parameters (NLM), using both simulated and real data. BFM is shown to be more stable than NLM at the voxel level and is computationally much faster. Application of the technique is illustrated for three radiotracers: [^{11}C]raclopride (a marker of the D2 receptor), [^{11}C]SCH 23390 (a marker of the D1 receptor) in human studies, and [^{11}C]CFT (a marker of the dopamine transporter) in rats. The assumptions implicit in the model and its implementation using BFM are discussed.

INTRODUCTION

This paper considers the evolution of a reference region model for the quantification of radioligand–receptor binding in the brain using positron emission tomography (PET) and shows how this development allows for a robust voxel by voxel implementation yielding parametric images of binding potential (*BP*; Mintun *et al.*, 1984), and the local rate of delivery of the radioligand relative to the reference region (R_1).

Parametric imaging of compartmental models in PET is often compromised by two factors. First, a high degree of parameterization in the model can lead to numerically unidentifiable parameter estimates, and second, optimization using conventional nonlinear least squares methods is both time-consuming and prone to local minima. These issues, which are particularly important at the voxel level, are addressed in this paper.

The present work employs a simplified reference region model (Lammertsma and Hume, 1996) involving only three parameters: *BP*, R_1, and k_2 (the effective efflux rate constant from the tissue) and introduces a basis function approach, including parameter bounds, to its solution. An algorithm enabling a fast and robust implementation of this model on a voxel by voxel basis is presented and the method is applied to three PET ligands: [^{11}C]raclopride (a marker of the D2 receptor) and [^{11}C]SCH 23390 (a marker of the D1 receptor) in humans and [^{11}C]CFT (a marker of the dopamine transporter) in rats.

THEORY

Background

The reference region model described by Blomqvist *et al.* (1989) and by Cunningham *et al.* (1991) relies on the existence of a tissue region with a negligible concentration of specific (saturable) binding sites. Under tracer conditions, formulation of this model involves six rate constants: K_1, k_2, K'_1, k'_2, describing the exchange of tracer between plasma and free (plus nonspecifically bound) ligand compartments in the region of interest and the reference region respectively, and k_3, k_4, describing the exchange of tracer between the free compartment and a specifically bound ligand compartment in the region of interest. By using the reference region to describe the kinetics of the free ligand, and assuming that the degree of nonspecific binding is the same in both regions, the kinetics of the ligand in tissue regions of interest displaying specific binding may then be described as a function of the reference region. This removes the need for a metabolite-corrected plasma input function. Under tracer conditions this formulation has five identifiable parameters groupings: $R_1 = K_1/K'_1$, k'_2, k_2, k_3, k_4 (Cunningham *et al.*, 1991; Gunn, 1996). Under the further assumption that the volume of distribution of the free compartment is the same in both regions (i.e., $K_1/k_2 = K'_1/k'_2$) the number of parameters required is reduced to four: R_1, k_2, k_3, k_4 (Cunningham *et al.*, 1991; Hume *et al.*, 1992). This formulation has been validated for [^{11}C]diprenorphine in the rat by comparison with data obtained *in vitro* (Cunningham *et al.*, 1991) and for [^{11}C]raclopride in humans by compari-

1053-8119/97 $25.00

son with the equivalent plasma input model (Lammertsma *et al.*, 1996). In these cases there is a finite rate of exchange between the free and the specifically bound compartments. Lammertsma and Hume (1996) introduced an additional simplification to the model which can be applied to ligands for which the exchange between the free and the specifically bound compartments is sufficiently rapid. In these cases the tissue region of interest may be approximated by a single compartment. This reduces the number of parameters required to three (R_I, k_2, BP), where BP is the binding potential (c.f. Mintun *et al.*, 1984). Here we define $BP = k_3/k_4$. Under tracer conditions $k_3/k_4 = B_{\max} f_2/(K_{D_{\text{Tracer}}}(1 + \Sigma_i(F_i/K_{D_i})))$, where $B_{\max}$ is the total concentration of specific binding sites, $K_{D_{\text{Tracer}}}$ is the equilibrium disassociation constant of the radioligand, f_2 is the "free fraction" of the unbound radioligand in the tissue, and F_i and K_{D_i} are the concentration and equilibrium disassociation constants of i competing endogenous ligands.

The simplified reference region model has the following operational equation,

$$C_T(t) = R_I C_R(t) + \left\{k_2 - \frac{R_I k_2}{1 + BP}\right\} C_R(t) \otimes e^{-[(k_2/(1+BP)+\lambda]t} \quad (1)$$

where $C_R(t)$ is the concentration time course in the reference region, $C_T(t)$ is the concentration time course in the tissue region of interest, k_2 is the (effective) efflux rate constant from the tissue, R_I is the ratio of the delivery in the tissue region of interest compared to that in the reference region (ratio of influx), and λ is the physical decay constant of the isotope. $\otimes$ is the convolution operator. Note that the above formulation refers to nondecay corrected data (see later).

This model has been validated and applied successfully on a region of interest (ROI) basis (Lammertsma and Hume, 1996). However, application of this model at the voxel level using a conventional nonlinear least squares approach to parameter estimation is slow and sensitive to noise. This problem is addressed in the present paper as follows.

Formulation

The simplified reference region model may be rewritten as,

$$C_T(t) = \theta_1 C_R(t) + \theta_2 C_R(t) \otimes e^{-\theta_3 t} \quad (2)$$

where $\theta_1 = R_I$, $\theta_2 = k_2 - R_I k_2/(1 + BP)$, and $\theta_3 = k_2/(1 + BP) + \lambda$.

This equation is linear in θ_1 and θ_2. Hence for fixed values of θ_3, θ_1 and θ_2 can be estimated using standard linear least squares. The nonlinear term can be dealt with by choosing a discrete spectrum of parameter values for θ_3 (see below) and forming the corresponding basis functions;

$$B_i(t) = C_R(t) \otimes e^{-\theta_{3_i} t} \quad (3)$$

Equation (2) can then be transformed into a linear equation for each basis function,

$$C_T(t) = \theta_1 C_R(t) + \theta_2 B_i(t) \quad (4)$$

Equation (4) is then solved using linear least squares for each basis function. The index i for which the residual sum of squares is minimized is determined by a direct search and the associated parameter values for this solution are obtained (θ_1, θ_2, θ_3). Values for BP, R_I, and k_2 are then easily deduced from the relationships given in equation (2).

A logarithmic range of values for θ_3 can be selected to encompass all plausible values for this parameter as governed by k_2, BP, and λ. This allows the introduction of parameter bounds on θ_3;

$$\lambda < \theta_3^{\min} \le \theta_{3_i} \le \theta_3^{\max}, \qquad i = 1, \ldots, 100 \quad (5)$$

where $\theta_3^{\min} \le k_2^{\min}/(1 + BP^{\max}) + \lambda$ and $\theta_3^{\max} \ge k_2^{\max} + \lambda$. For the ligands considered in this paper 100 discrete values for θ_3 were found to be sufficient with $\theta_3^{\min} = 0.001 s^{-1}$ and $\theta_3^{\max} = 0.01 s^{-1}$.

Algorithm

A fast algorithm for the basis function method (BFM) is obtained by performing as many of the calculations as possible before considering the individual voxel time courses. Weighted least squares solutions are obtained by employing a QR decomposition of the reference region with each of the basis functions separately. The algorithm is summarized below in pseudo-code;

Initially

$C_R(t)$	measured reference region time course
$B_i(t) = C_R(t) \otimes e^{-\theta_{3_i} t}$	basis functions, $i = 1, \ldots, 100$
$w = \dfrac{(\text{frame duration})^2}{\text{total counts in frame}}$	weights
$W = \text{diag}(\sqrt{w})$	weighting matrix
For i = 1:100	
	$A = [C_R \quad B_i]$
	$[Q, R] = qr(W.A)$
	$M(2i - 1{:}2i, :) = R \backslash Q^T$
end	

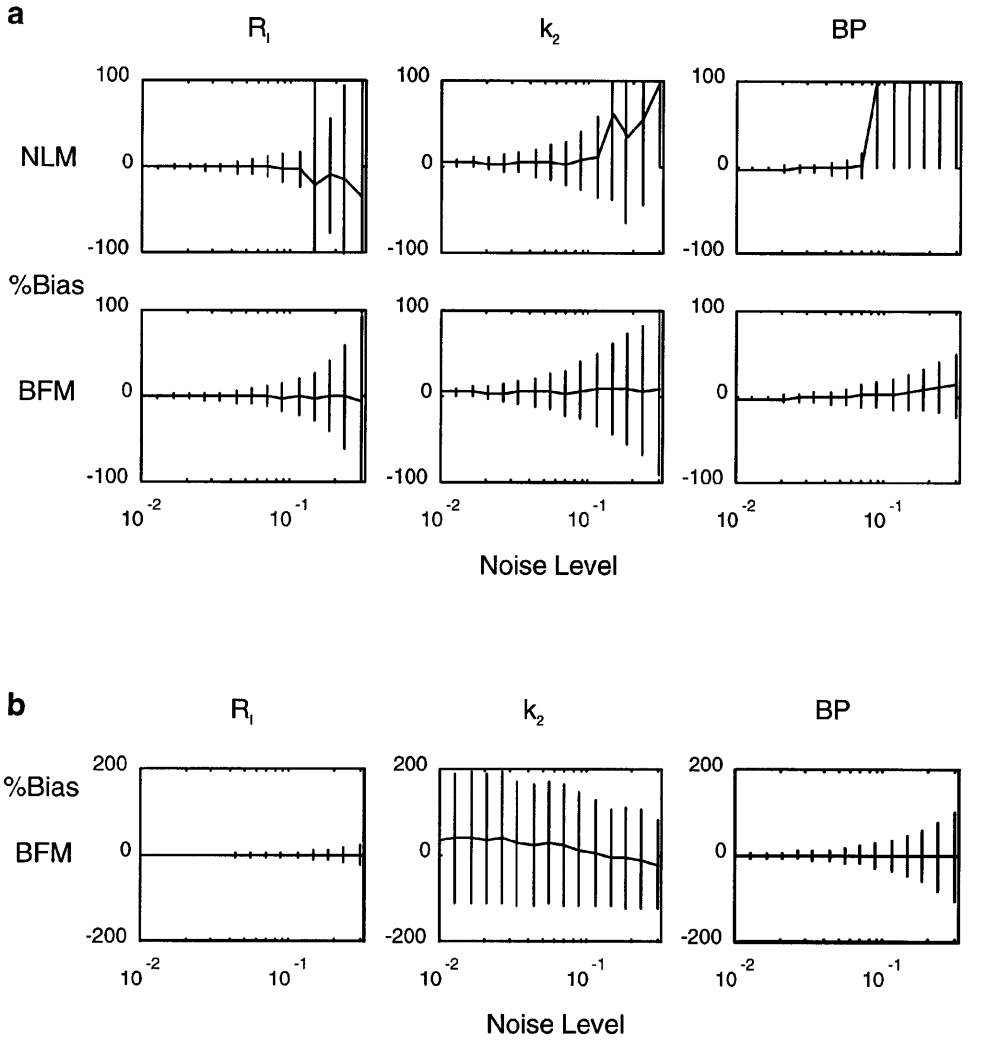

FIG. 1. Simulations of bias in BFM and NLM for different noise levels: (a) $R_I = 1.2$, $k_2 = 0.0024\text{s}^{-1}$, and $BP = 2$, (b) $R_I = 1.2$, $k_2 = 0.0024\text{s}^{-1}$, and $BP = 0.2$.

where $m = R \backslash Q^T$ is the solution in the least squares sense to the overdetermined system of equations $Rm = Q^T$.

For each voxel

$C_{\text{PET}}(t_j)$ measured concentration at time t_j.

$j = 1, \ldots, n$, where n is the number of frames

For $i = 1{:}100$

$$\begin{bmatrix}\theta_1\\ \theta_2\end{bmatrix} = M(2i - 1{:}2i, :).W.C_{\text{PET}}(t_j)$$

$$C_T(t_j) = \theta_1 C_R(t_j) + \theta_2 B_i(t_j)$$

$$RSS_i = \sum_{j=1}^{n} w.(C_{\text{PET}}(t_j) - C_T(t_j))^2$$

end

$$i_{\min} = \text{find}(\min(RSS_i))$$

$$\begin{bmatrix}\theta_1\\ \theta_2\end{bmatrix} = M(2i_{\min} - 1{:}2i_{\min}, :).W.C_{\text{PET}}(t_j)$$

$$R_I = \theta_1$$

$$k_2 = \theta_2 + R_I(\theta_3 - \lambda)$$

$$BP = \frac{k_2}{\theta_3 - \lambda} - 1$$

METHODS

Simulations

Monte Carlo simulations were carried out in order to compare the behavior of the BFM with a conventional

nonlinear least squares method (NLM) in the presence of noise. Perfect reference and tissue data were generated with the model, using a metabolite-corrected plasma input function obtained from a human [^{11}C]-raclopride study with continuous blood sampling, discrete measures of plasma and whole blood activity, discrete plasma metabolites assays as described by Lammertsma *et al.* (1996), and by choosing parameter values for both a high and low binding region ($R_I = 1.2$, $k_2 = 0.0024\text{s}^{-1}$, $BP = 2$, and $R_I = 1.2$, $k_2 = 0.0024\text{s}^{-1}$, $BP = 0.2$, respectively). Noisy data were then obtained by adding normally distributed noise to the perfect data. The simulations were performed for a typical study protocol of 17 frames over a period of 1 h (1×15, 1×5, 1×10, 1×30, 4×60, 3×300, 2×600, 4×300 s). A lower level of noise was added to the reference data than the tissue data (noise in tissue = $20 \times$ noise in reference region) to simulate a situation where the reference data obtained from a larger region of interest is smoother than the voxel data. The normally distributed noise was scaled such that 1 standard deviation corresponded to the maximum count in each simulated curve (i.e., 1 corresponds to a very high noise level). 1000 realizations were produced for all the simulations at each different noise level. Data were analyzed using BFM as described above. For NLM a simplex method was employed to minimize the weighted residual sums of squares (Nelder and Mead, 1965).

The sensitivity of the estimated binding potential to the presence of specific binding in the reference region was also investigated using noiseless simulated data. These simulated results were compared with an explicit algebraic equation derived from a consideration of the ratio of the expected distribution volumes at equilibrium.

$$BP_{\text{Apparent}} = \frac{BP_{\text{Tissue}} + 1}{BP_{\text{Reference}} + 1} - 1 \qquad (6)$$

where $BP_{\text{Reference}}$ and BP_{Tissue} are the true binding potentials of the ligand in the reference and target tissues, respectively. BP_{Apparent} would be the binding potential estimated in the target tissue under the assumption that $BP_{\text{Reference}}$ is zero.

Human Studies

[^{11}C]Raclopride. Data were taken from an ongoing study (Dr P. Grasby, MRC Cyclotron Unit) for which ARSAC and local hospital approved ethics permission had been obtained. Four normal volunteers were scanned for 1 h after intravenous administration of [^{11}C]raclopride (Injected activity: 9.62, 9.28, 9.65, 9.73 mCi) using an ECAT 953B PET camera (CTI/Siemens, Knoxville, TN) which has been previously characterized (Spinks *et al.*, 1992). Dynamic data were acquired in 3D mode and 17 frames (1×15, 1×5, 1×10, 1×30, 4×60, 3×300, 2×600, 4×300 s) were collected. A convolution subtraction method was used for scatter correction (Bailey and Meikle, 1994) and a 3D reconstructed image was obtained using a reprojection algorithm (Kinahan and Rogers, 1989), which included a calculated attenuation correction. An ROI template was defined on an integral image (Sawle *et al.*, 1990; Bench *et al.*, 1993) and applied to the dynamic images to produce time radioactivity curves corresponding anatomically to cerebellum (reference region), caudate, putamen, left caudate, right caudate, left anterior putamen, right anterior putamen, left mid putamen, right mid putamen, left posterior putamen, right posterior putamen, frontal cortex, occipital cortex, and thalamus.

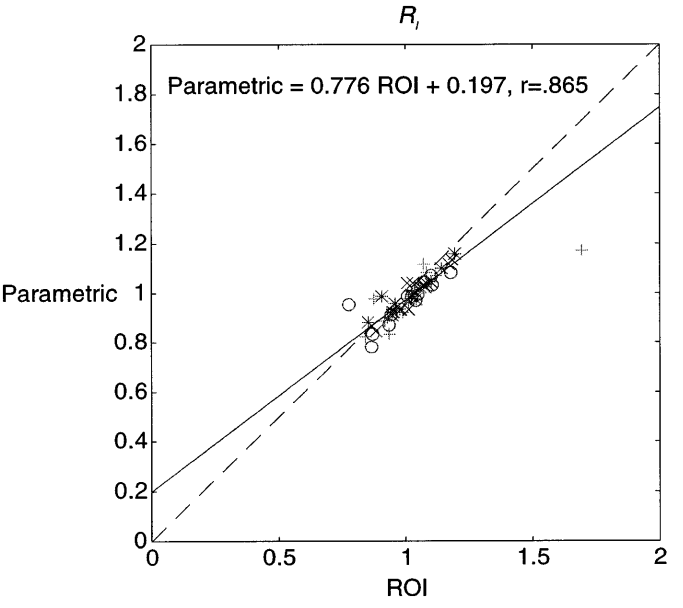

FIG. 2. Human [^{11}C]raclopride: R_I values for the basis function parametric image method versus the nonlinear ROI method (Different symbol for each study).

[^{11}C]SCH 23390. Data were taken from an ongoing study (Dr. T. Andrews, MRC Cyclotron Unit) for which ARSAC and local hospital approved ethics permission had been obtained. A single [^{11}C]SCH 23390 scan was acquired using an identical protocol to the [^{11}C]raclopride scan described above (Injected activity: 10.64 mCi).

Rat Studies

[^{11}C]CFT. A small animal scanner built in collaboration with CTI PET systems (Knoxville, TN) was used to scan 11 adult male Sprague–Dawley rats while anesthetized. The work was carried out by licensed investigators in accordance with the Home Office's "Guidance on the Operation of Animal (scientific Procedures) Act 1986" (HMSO, Feb 1990). The scanner has a diameter

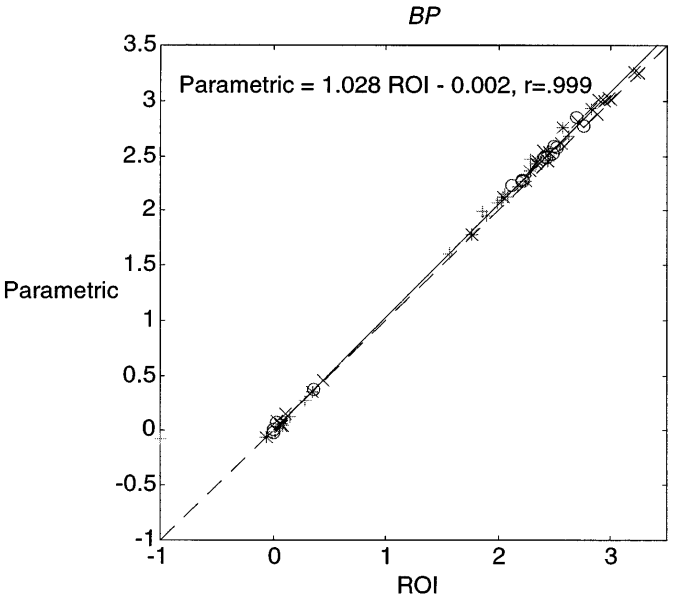

FIG. 3. Human [^{11}C]raclopride: *BP* values for the basis function parametric image method versus the nonlinear ROI method (Different symbol for each study).

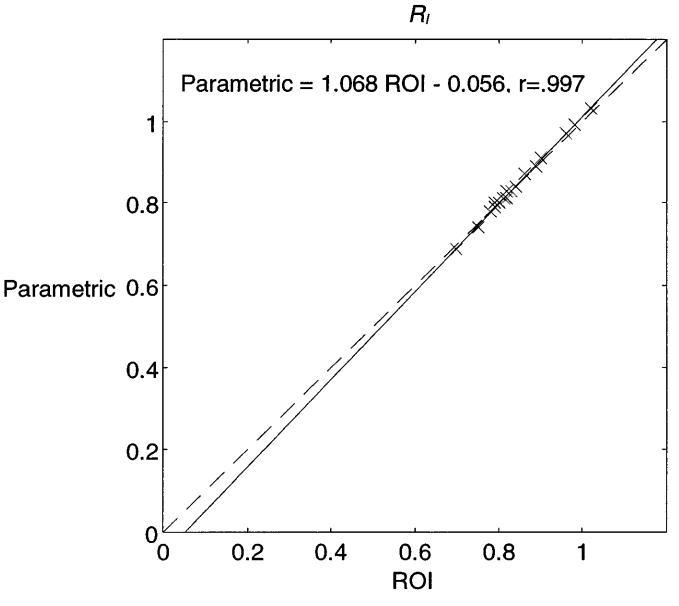

FIG. 4. Rat [^{11}C]CFT: R_I values for the basis function parametric image method versus the nonlinear ROI method.

of 11.5 cm and an axial field of view of 5 cm and its physical characteristics have been described previously (Bloomfield *et al.*, 1995). Dynamic data were acquired in 3D mode (Bloomfield *et al.*, 1997) and 21 frames of data (3×5, 3×15, 4×60, 11×300 s) were collected. [^{11}C]CFT was administered as a bolus via a catheter previously implanted in a lateral vein of the tail (range 196–365 μCi). Different specific activities (equivalent to cold doses in the range 0.30–8178 nmol.(kg body weight)$^{-1}$) were injected so as to give a range of binding potential values. The dynamic images were reconstructed using filtered back projection (Kinahan and Rogers, 1989) and these images were subsequently interpolated to give cubic voxels, using Analyze software (Robb and Hanson, 1991). An ROI template (Myers *et al.*, 1996) was defined on an integral image and applied to the dynamic images to produce time radioactivity curves corresponding anatomically to the

TABLE 1

R_I and *BP* Values for Various Anatomical Regions from Four Human [^{11}C]Raclopride Studies

	Human [^{11}C]raclopride studies															
Study	1				2				3				4			
Parameter	R_I		*BP*		R_I		*BP*		R_I		*BP*		R_I		*BP*	
Method	ROI	PAR	ROI	PAR	ROI	PAR	ROI	PAR	ROI	PAR	ROI	PAR	ROI	PAR	ROI	PAR
Caudate	0.93	0.90	2.03	2.10	1.03	0.99	2.71	2.81	0.94	0.91	2.48	2.52	1.14	1.10	2.29	2.36
Putamen	1.01	0.96	2.06	2.15	1.07	1.02	2.95	3.00	1.04	0.97	2.41	2.50	1.02	0.99	2.34	2.43
L. Caudate	0.84	0.82	2.08	2.13	1.07	1.04	2.89	3.01	0.87	0.84	2.43	2.48	1.19	1.16	2.35	2.45
R. Caudate	1.01	0.98	1.99	2.08	0.98	0.94	2.55	2.61	1.01	0.99	2.52	2.57	1.09	1.04	2.24	2.27
L. Ant. Put	0.99	0.93	1.57	1.60	0.95	0.91	3.00	3.02	1.10	1.07	2.50	2.58	1.06	1.02	2.83	2.93
R. Ant. Put	0.92	0.89	1.90	1.95	1.18	1.13	3.25	3.25	1.05	1.00	2.21	2.28	0.96	0.96	2.44	2.46
L. Mid. Put	1.04	1.00	2.18	2.22	1.06	1.02	3.21	3.27	1.10	1.04	2.70	2.85	1.10	1.05	2.46	2.54
R. Mid. Put	1.06	1.02	2.63	2.68	1.07	1.03	2.99	3.03	1.18	1.08	2.76	2.77	1.04	0.97	2.58	2.76
L. Post. Put	1.12	1.07	1.86	1.99	1.17	1.12	2.87	2.87	0.87	0.79	2.12	2.23	0.95	0.92	1.76	1.78
R. Post. Put	0.94	0.83	2.29	2.47	1.01	0.94	2.40	2.55	0.93	0.87	2.21	2.26	1.02	1.00	2.04	2.13
Front. Ctx	1.08	1.08	−1.00	−0.07	1.01	1.04	0.08	0.05	1.07	1.05	0.01	0.01	0.85	0.88	−0.06	−0.06
Occip. Ctx	1.70	1.17	0.02	−0.01	20.6	1.07	0.04	0.08	1.04	0.99	0.03	0.07	0.95	0.92	0.08	0.05
Thalamus	0.88	0.98	0.15	0.12	0.88	0.85	0.12	0.15	0.78	0.95	0.00	−0.02	0.91	0.99	0.08	0.05
All	1.07	1.12	0.28	0.28	1.03	1.04	0.44	0.46	1.02	0.99	0.36	0.38	0.98	0.94	0.34	0.35

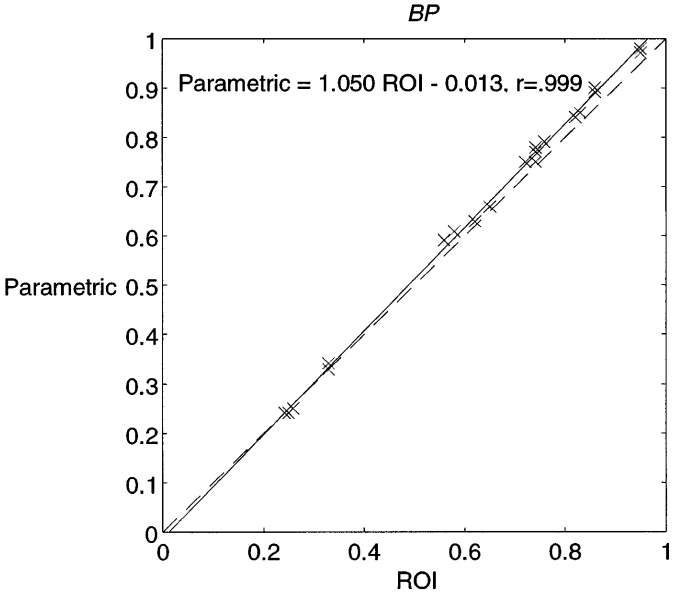

FIG. 5. Rat [^{11}C]CFT: *BP* values for the basis function parametric image method versus the nonlinear ROI method.

TABLE 2

R_1 and *BP* Values for Right Striatum (RS) and Left Striatum (LS) from 11 Rat [^{11}C]CFT Studies

	Rat [^{11}C]CFT studies							
	ROI				Parametric			
	R_1		*BP*		R_1		*BP*	
Study	RS	LS	RS	LS	RS	LS	RS	LS
1	0.79	0.81	0.74	0.82	0.80	0.81	0.77	0.84
2	0.90	1.02	0.86	0.95	0.91	1.03	0.90	0.98
3	0.83	0.81	0.83	0.86	0.83	0.81	0.85	0.89
4	0.82	0.81	0.33	0.33	0.81	0.81	0.33	0.34
5	0.78	0.82	0.65	0.62	0.78	0.83	0.66	0.63
6	0.89	0.86	0.86	0.95	0.89	0.87	0.90	0.97
7	0.96	0.98	0.56	0.58	0.97	0.99	0.59	0.61
8	0.82	0.83	0.74	0.76	0.83	0.83	0.78	0.79
9	0.70	0.75	0.24	0.25	0.69	0.74	0.24	0.24
10	0.84	0.80	0.74	0.72	0.84	0.80	0.75	0.75
11	0.79	0.78	0.26	0.24	0.79	0.78	0.25	0.24

cerebellum (reference region), right striatum, and left striatum.

Both the [^{11}C]raclopride and [^{11}C]CFT data sets were analyzed on a ROI level using NLM (Lammertsma and Hume, 1996) and on a voxel by voxel basis using the BFM described above.

RESULTS

The present method (BFM) was developed in order to implement the simplified reference region model at the voxel level. This model has previously been validated using time activity data derived from large ROIs, with correspondingly less noise, employing conventional nonlinear least squares for parameter estimation (NLM). It will be seen later that NLM cannot be applied at the voxel level. In order to compare BFM with NLM, studies were therefore carried out using both simulated and real data. A comparison based on simulated human [^{11}C]raclopride studies is presented first.

The performance of the two methods as a function of noise in the simulated data is illustrated in Fig. 1. By considering the simulations for a high binding area (Fig. 1a) this shows that for low noise levels (up to 0.1) there was essentially no difference between the two methods in terms of bias or variance. In this case the estimates obtained by the NLM for θ_3 all lie within the range of values corresponding to the basis functions chosen for the BFM. However, when the noise level exceeded 0.1, the NLM was unstable and gave unreasonably large values for *BP*. This problem is avoided with the BFM due to the parameter bounds introduced on the exponential term (see Theory). At these higher noise levels a corresponding bias becomes apparent in the BFM. However, the bias introduced is small even at high noise levels. When considering the simulations for the low binding area (Figure 1b) the NLM was unable to find a solution, even for low noise levels. This can be explained by the fact that the parameter k_2 becomes numerically unidentifiable in this case. The BFM, however, is robust due to the inclusion of the parameter bounds. The variance in the *BP* parameter estimate is increased slightly and there is still no significant bias. The large variance in k_2 illustrates that this parameter is often numerically unidentifiable and that parameter bounds are essential.

When comparing the performance of the two methods on real data it was therefore necessary to apply the NLM to the average time activity curves derived from whole ROIs, whereas the BFM could be applied at the voxel level. The resultant voxel parameter estimates from the BFM were therefore averaged over the ROIs for comparison with NLM. The correspondence be-

FIG. 6. Human [^{11}C]raclopride study: Parametric images of R_1 and *BP* from a representative midtransaxial plane using the basis function method presented.

FIG. 7. Rat [^{11}C]CFT: Parametric images of R_1 and *BP* from a horizontal plane at the level of the striatum using the basis function method presented.

FIG. 8. Human [^{11}C]SCH 23390 study: Parametric images of R_1 and *BP* from a representative midtransaxial plane using the basis function method presented.

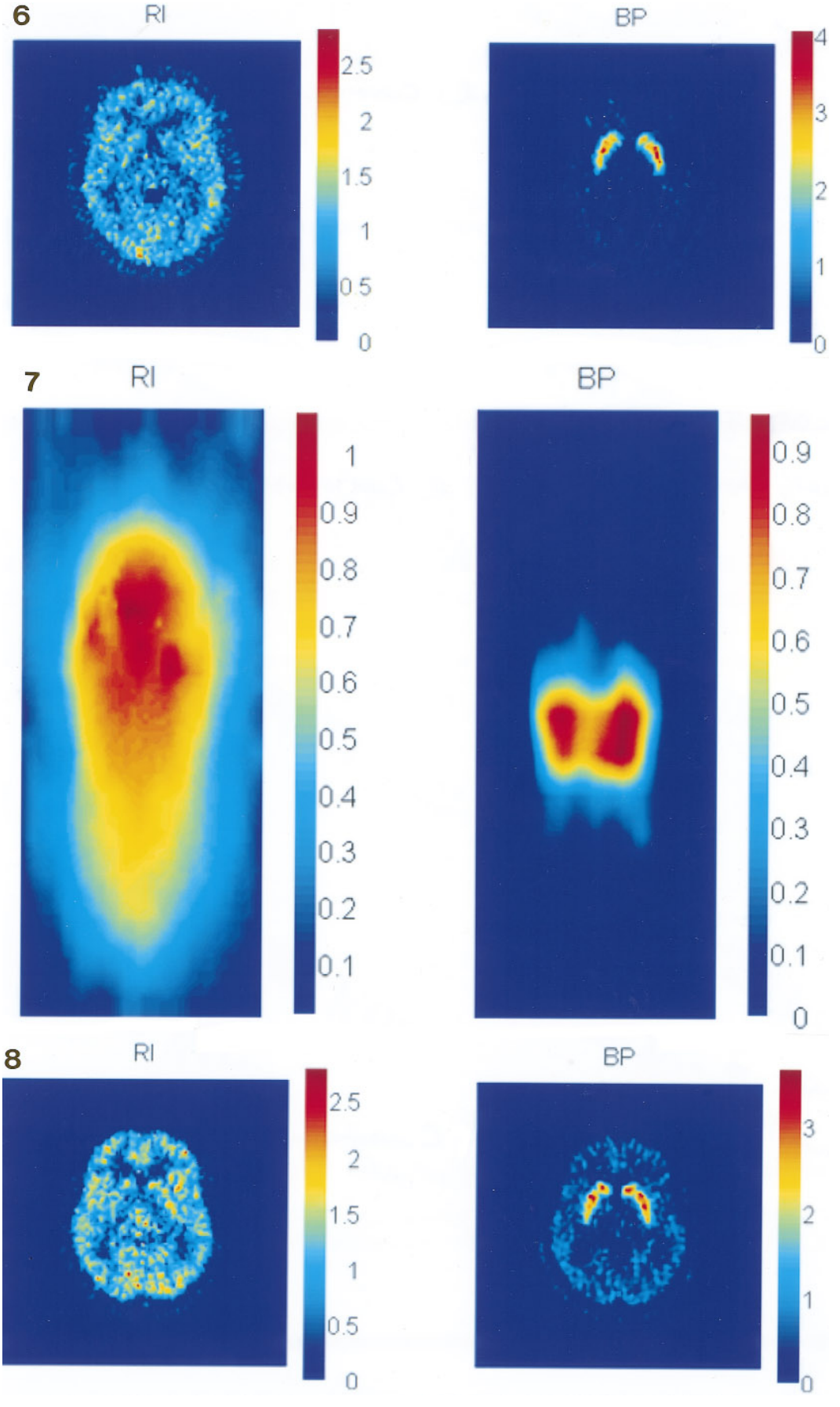
6
RI
2.5
2
1.5
1
0.5
0
BP
4
3
2
1
0
7
RI
1
0.9
0.8
0.7
0.6
0.5
0.4
0.3
0.2
0.1
BP
0.9
0.8
0.7
0.6
0.5
0.4
0.3
0.2
0.1
0
8
RI
2.5
2
1.5
1
0.5
0
BP
3
2
1
0

tween the two methods is illustrated for four [^{11}C]raclopride studies in humans in Figs. 2 and 3 and the values tabulated in Table 1. These results show that the parametric images are well correlated with the previously validated estimates of BP and R_I obtained for ROIs using NLM.

Figures 4 and 5, together with Table 2 give the corresponding data obtained from [^{11}C]CFT studies in rats. Again, good agreement was obtained between the two methods. Note, only striatal regions were considered in these studies.

Representative parametric images obtained using the basis function approach for [^{11}C]raclopride and [^{11}C]CFT are illustrated in Figs. 6 and 7. The applicability of the simplified reference region model to [^{11}C]SCH 23390 has already been validated at the ROI level (Lammertsma and Hume, 1996). Its application at the voxel level using BFM is illustrated in Fig. 8. For human data the method takes approximately 1 min per plane (128 $\times$ 128 voxels) on a sparc Ultra computer.

The sensitivity of the estimated binding potential in the target tissue to the assumption of no specific binding in the reference tissue was investigated using simulated data as described under Methods. The consequent underestimation of the true binding potential in the target tissue conformed exactly with the theoretical Eq. (6).

DISCUSSION

A method has been presented which allows parametric imaging of both binding potential and the delivery of the ligand relative to the reference region which requires only tomographic tissue data. The principle advantages of the method are robustness and computational speed.

The robustness derives in part from the small number of parameters (3) in the model. However, this formulation involves several major assumptions; a reference region exists and can be defined. Labeled metabolites of the parent tracer do not cross the blood–brain barrier. The degree of nonspecific binding, and the ratio of the rate constants describing the exchange of tracer between plasma and the free/nonspecific compartment are the same in both tissue and reference regions. The exchange between free and specifically bound compartments is sufficiently fast for their composite behavior to be approximated by a single compartment. Clearly the applicability of these assumptions needs to be taken in account before applying the current method to the analysis of dynamic PET data. In particular attention is drawn to Eq. (6) which describes the sensitivity of the estimates of binding potential to the assumption that the reference tissue is devoid of specific binding. This equation allows for an estimate of the resulting bias if independent data on the specific binding in the reference region is available.

Despite the improvement in stability associated with the reduction in the number of parameters in the reference tissue model from 4 to 3 (Lammertsma and Hume, 1996), additional constraints are required for its implementation at the voxel level. In the present work the robustness of the BFM is achieved by the introduction of parameter bounds in the estimation problem and by the direct search for the global minimum. This is readily enabled by its formulation in terms of basis functions. The parameter bounds are based on *a priori* knowledge of the ligands' behavior, which can be sensibly obtained from previous ROI analyses. The parameter bounds are particularly important when the method is applied to target regions displaying relatively low binding potential and the shape and scale of the reference and target time activity curves are similar. In this case the estimate of k_2 becomes numerically unidentifiable as can be seen by inspection of Eq. (1). Propagation of this effect to the estimates of BP and R_I is minimized by the imposition of parameter bounds.

The introduction of parameter bounds will in general be accompanied by an associated bias. In the examples presented, the bias in the principle parameter of interest, BP, was negligible. However, this property of the method should be investigated in individual applications particularly when the behavior of the ligand approaches irreversibility within the time course of the PET scan.

The computational speed derives from the predefined basis functions being linear in the parameters (θ_1, θ_2). The nonlinear parameter, θ_3, is accommodated by a direct search across the basis functions which guarantees a global minimum within the constraints. This approach using linear least squares together with a discretised range of basis functions incorporating the nonlinearity and covering the expected physiological range was introduced by Koeppe *et al.* (1985) to the quantitation of local cerebral blood flow using a blood input function and the Kety model.

Recently, a method for the estimation of distribution volume ratios using a reference tissue without blood sampling has been proposed by Logan *et al.* (1996). This graphical method does not require the assumption of rapid exchange between the compartments in the target tissue but does require an *a priori* estimate of the efflux rate constant in the reference region (k'_2) and also the identification of the linear portion of the graph. The present BFM method involves fitting the total untransformed dataset obtained from the target tissue. This requires no arbitrary temporal partitioning of the dataset and facilitates appropriate statistical weighting.

In addition to parametric imaging of BP, the BFM method also allows generation of parametric images of R_I and k_2. The R_I images, in particular, provide a useful

adjunct to the specific ligand binding images. It would be expected that the R_1 image would be dominated by relative regional blood flow. In protocols involving repeat scans this provides an independent assessment of any regional changes in delivery. In addition the R_1 images can be used for coregistration purposes as they provide good structural information. For data such as [^{11}C]raclopride, the specific binding of which is concentrated in the striatum, the transformation parameters derived from R_1 images can allow for coregistration or stereotactic normalization which can also be applied to the *BP* images. This will facilitate the statistical analysis at the voxel level of changes in both the delivery and binding of neuroligands.

ACKNOWLEDGMENTS

We thank Ralph Myers, Julian Matthews, Paul Grasby, Thomasin Andrews, Peter Bloomfield, and Ella Hirani for the provision of data and for useful discussions.

REFERENCES

Bailey, D. L., and Meikle, S. R. 1994. A convolution-subtraction scatter correction method for 3D PET. *Phys. Med. Biol.* **39:**411–424.

Bench, C. J., Lammertsma, A. A., Dolan, R. J., Grasby, P. M., Warrington, S. J., Gunn, K., Cuddigan, M., Turton, D. J., Osman, S., and Frackowiak, R. S. J. 1993. Dose dependent occupancy of central dopamine D_2 receptors by the novel neuroleptic CP-88,059-01: A study using positron emission tomography and ^{11}C-raclopride. *Psychopharmacology* **112:**308–314.

Blomqvist, G., Pauli, S., Farde, L., Ericksson, L., Persson, A., and Halldin, C. 1989. Dynamic models of reversible ligand binding. In *Clinical Research and Clinical Diagnosis* (C. Beckers, A. Goffinet, and A. Bol, Eds). Kluwer Academic Publishers.

Bloomfield, P. M., Rajeswaran, S., Spinks, T. J., Hume, S. P., Myers, R., Ashworth, S., Clifford, K. M., Jones, W. F., Byars, L. G., Young, J., Andreaco, M., Williams, C. W., Lammertsma, A. A., and Jones, T. 1995. Design and physical characteristics of a small animal positron emission tomograph. *Phys. Med. Biol.* **40:**1105–1126.

Bloomfield, P. M., Myers, R., Hume, S. P., Spinks, T. J., Lammertsma, A. A., and Jones, T. 1995. Three-dimensional performance of a small-diameter positron emission tomograph. *Phys. Med. Biol.* **42:**389–400.

Cunningham, V. J., Hume, S. P., Price, G. R., Ahier, R. G., Cremer, J. E., and Jones, A. K. P. Compartmental analysis of diprenorphine binding to opiate receptors in the rat in vivo and its comparison with equilibrium data in vitro. *J. Cereb. Blood Flow Metab.* **11:**1–9.

Gunn, R. N. 1996. Mathematical modelling and identifiability applied to positron emission tomography data. Ph.D. Thesis, University of Warwick.

Hume, S. P., Myers, R., Bloomfield, P. M., Opacka-Juffry, J., Cremer, J. E., Ahier, R. G., Luthra, S. K., Brooks, D. J., and Lammertsma, A. A. 1992. Quantitation of carbon-11-labeled raclopride in rat striatum using positron emission tomography. *Synapse* **12:**47–54.

Kinahan, P. E., and Rogers, J. G. 1989. Analytic 3-D image reconstruction using all detected events. *IEEE Trans. Nucl. Sci.* **NS-36:**964–968.

Koeppe, R. A., Holden, J. E., and Ip, W. R. 1985. Performance comparison of parameter estimation techniques for the quantitation of local cerebral blood flow by dynamic positron computed tomography. *J. Cereb. Blood Flow Metab.* **5:**224–234.

Lammertsma, A. A., Bench, C. J., Hume, S. P., Osman, S., Gunn, K., Brooks, D. J., and Frackowiak, R. S. J. 1996. Comparison of methods for analysis of clinical [^{11}C]raclopride studies. *J. Cereb. Blood Flow Metab.* **16:**42–52.

Lammertsma, A. A., and Hume, S. P. 1996. Simplified reference tissue model for PET receptor studies. *NeuroImage* **4:**153–158.

Logan, J., Fowler, J. S., Volkow, N. D., Wang, G-J., Ding, Y-S., and Alexoff, D. L. 1996. Distribution volume ratios without blood sampling from graphical analysis of PET data. *J. Cereb. Blood Flow Metab.* **18:**834–840.

Mintun, M. A., Raichle, M. E., Kilbourn, M. R., Wooten, G. F., and Welch, M. J. 1984. A quantitative model for the in vivo assessment of drug binding sites with positron emission tomography. *Ann. Neurol.* **15:**217–227.

Myers, R., Hume, S. P., Ashworth, S., Lammertsma, A. A., Bloomfield, P. M., Rajeswaran, S., and Jones, T. 1996. Quantification of dopamine receptors and transporter in rat striatum using a small animal PET scanner. In *Quantification of Brain Function Using PET* (R. Myers, V. J. Cunningham, D. L. Bailey, and T. Jones, Eds). Academic Press, San Diego.

Nelder, J. A., and Mead, R. 1965. A simplex method for function minimization. *Comput. J.* **7:**308–313.

Robb, R. A., and Hanson, D. P. 1991. A software system for interactive and quantitative visualization of multidimensional biomedical images. *Austral. Phys. Eng. Sci. Med.* **14:**9–30.

Sawle, G. V., Colebatch, J. G., Shah, A., Brooks, D. J., Marsden, C. D., and Frackowiak, R. S. J. 1990. Striatal function in normal aging: Implications for Parkinson's disease. *Ann Neurol.* **28:**799–804.

Spinks, T. J., Jones, T., Bailey, D. L., Townsend, D. W., Grootoonk, S., Bloomfield, P. M., Gilardi, M.-C., Casey, M. E., Sipe, B., and Reed, J. 1992. Physical performance of a positron tomograph for brain imaging with retractable septa. *Phys. Med. Biol.* **37:**1637–1655.